17th World Conference on Earthquake Engineering, 17WCEE
Sendai, Japan - September 13th to 18th 2020

SIMPLE MODELING METHOD OF BUILDING WITH CONTINUOUS ARRANGEMENT OF HYSTERETIC AND VISCOUS DAMPERS

K. Soeta [1], D. Sato [2], M. Ishii [3], H. Kitamura [4]

[1] *Structural Engineer Division, KUME SEKKEI Ltd., kohei.soeta@kumesekkei.co.jp*
[2] *Assoc. Prof., FIRST, Tokyo Institute of Tech., sato.d.aa@m.titech.ac.jp*
[3] *Structural Design Division, Nikken Sekkei Ltd., ishiim@nikken.jp*
[4] *Vice President, Tokyo Univ. of Science, kita-h@rs.noda.tus.ac.jp*

Abstract

Seismic control has become generally used in super tall steel structure buildings. A combination of hysteretic dampers and viscous dampers is increasingly used nowadays to ensure high earthquake resistance of high-rise buildings – as such, this is called a "combination-system". In design of buildings, simple model such as equivalent shear spring model is frequently used. However, there is no current research on simple model of "combination-system", thus, this paper proposes a method to create an equivalent shear-spring model of "combination-system" consisting of its characteristic values, dampers and their support members, and frames.

In creating the shear spring model, the parameters are calculated by conducting static analysis of the building frame in four states – (i) state *N* for frame only state, (ii) state *R* in which an elastic spring with extremely high rigidity is placed in the damper's installation position, (iii) state *pN* in which elastic springs are only placed in the hysteretic damper's installation stories, and (iv) state *pR* in which an elastic spring with extremely high rigidity is only placed in the hysteretic damper's installation position.

The parameters obtained from states *pN* and *pR* are important in evaluating seismic control effect of "combination-system". The obtained characteristic values from state *pN* show that the upper limit of the effective deformation ratio in the viscous damper's installation floor decreases. The obtained characteristic values from state *pR* show phase difference between the hysteretic damper load and viscous damper load.

A 30-storey high-rise building with brace-type continuous arrangement of hysteretic dampers and viscous dampers is used to verify the proposed model. A total of 13 damper placement combinations are used in this study. This paper shows that the proposed model reproduces the results of time-history analysis of member models. With respect to energy absorption of damper, the proposed model is more accurate than the previous models because the former evaluates various characteristic values and can reproduce the damper load at each step of the time-history analysis.

Keywords: seismic control, hysteretic damper, viscous damper, shear spring model, combination-system

1. Introduction

To reduce the deformation and damage of buildings against large earthquakes and unexpected earthquakes, it is typical to adopt seismic control structures for high-rise buildings in Japan.

In a high-rise building with a large bending deformation, the damping performance of middle to upper dampers may be deteriorated. To improve the deterioration of damping performance, the authors propose a "combination system," in which hysteretic dampers (HDs) and viscous dampers (VDs) are arranged in mixed stories [1]–[3].

When a designer examines the appropriate arrangement and quantity of dampers by time history response analysis, if time history response is relied upon significantly, the dampers may diverge owing to misalignment in the initial settings. This will result in a reduction effect and the loss of safety and comfort [4]. To avoid such a situation, it is necessary to perform a rough design using a response prediction method that can offer a comprehensive understanding of the relationship between the damper and response and to understand the damping performance from the index obtained in the process.

Hence, a simple model is required; however, research regarding the method of creating a simple model for the combination system has not been performed; therefore, the cumulative value, such as energy, is unknown.

Therefore, this paper presents a method for creating a simple model for the combination system. The simple model creation method proposed herein is an improvement of the method using the "characteristic values" proposed by Kasai/Iwasaki [5] and Ishii/Kasai [6] such that it can be applied to the combined model. The simple model is important because the member model is composed of a large number of members, such as columns, beams, and dampers that is reduced to a small number of characteristic values. Furthermore, the characteristic values reflect the damping performance and can be quantitatively evaluated on the same scale.

The definitions and expressions of terms used herein are as follows:

- The specifications of the i story are assigned the left subscript "*i*."
- The specifications of the simple model (spring system) are assigned the right subscript "*s*."
- The specification of the damper part is assigned a right subscript "*d*." In addition, the specifications of the brace type arranged in the direction of the diagonal axis indicate the converted value in the horizontal direction.

2. Extraction of problems using existing methods

2.1 Overview of existing methods [5] [6]

As shown in Fig. 1, the previous model is composed of a pseudo-frame, pseudo-brace, and pseudo-damper. The pseudo-brace and pseudo-damper are connected in series. The setting procedure for each item is described in Fig. 2. Fig.2(a) shows a model diagram of the combination system; Figs. 2(b) and 2(c) show conceptual diagrams of the state *N* analysis and *R* analysis of the previous method, and Figs. 2(d) and 2(e) show the conceptual diagram of the state *pN* analysis and *pR* analysis of the proposed method (Section 4, described later).

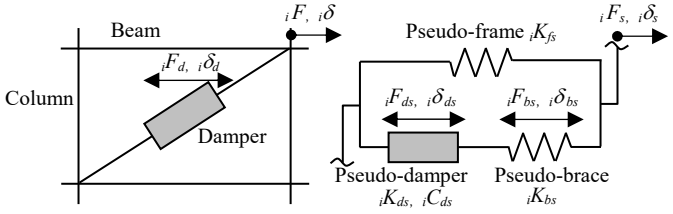

(a) Member model (b) Shear spring model

Fig.1 Correspondence between member model and shear spring model

The pseudo-frame stiffness ${}_iK_{fs}$ and the characteristic value ${}_i\alpha_N$ were calculated by conducting a static analysis of the building frame with the frame only (state *N*: no damper). The pseudo-brace stiffness ${}_iK_{bs}$ was calculated by conducting a static analysis of the building frame in which an elastic spring of extremely high rigidity was placed in the damper's installation position (state *R*: rigid damper). Each parameter was calculated by Eq. (1). Herein, the load in the static analysis is based on the Ai distribution, following [6].

$$ {}_i\alpha_N = {}_i\delta_{dN} / {}_i\delta_N,\ {}_iK_{bs} = {}_i\alpha_N \cdot {}_iK_{dR},\ {}_iK_{dR} = {}_iF_{dR} / {}_i\delta_R \quad (1a,b,c) $$

where ${}_iK_{dR}$ is the frame rigidity of the damper installation location; ${}_i\delta_d$ is the horizontal component of damper deformation; ${}_i\delta$ is the story drift of the frame; ${}_iF_d$ is the horizontal component of the axial force borne by the elastic spring at the damper installation location; the lower right subscripts *N* and *R* indicate the calculated values of states *N* and *R*, respectively.

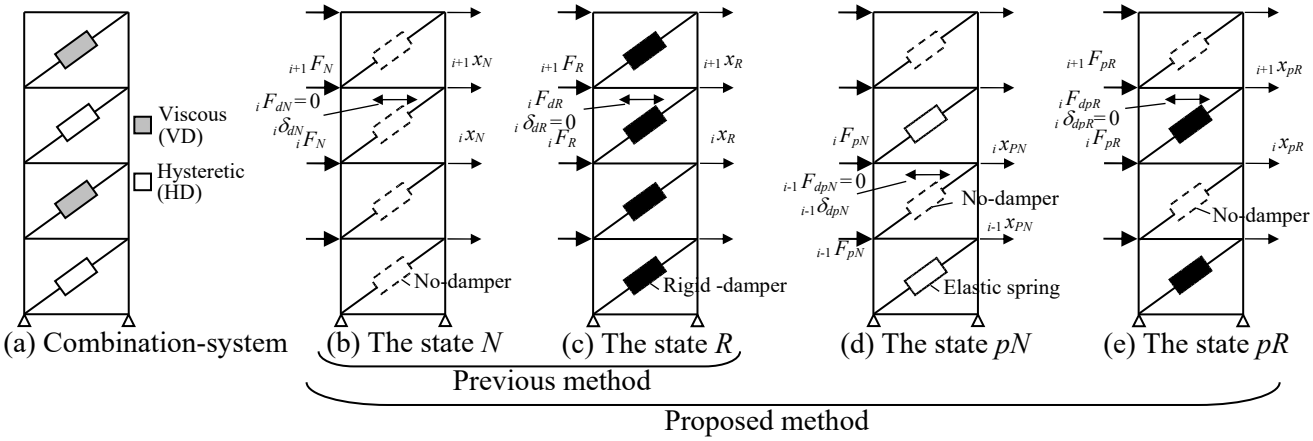

Fig.2 (a)Member model and the state (b)*N*, (c)*R*, (d)*pN* and (e)*pR*

Using these characteristic values, the specifications of the pseudo-frame, pseudo-brace, and pseudo-additional system are set as follows. The correspondence between the simple and member models is as follows.

◆Frame：

・Pseudo-frame rigidity ${}_iK_{fs} = {}_iK_N$ (2)

・Correspondence ${}_iF_s = {}_iF$, ${}_i\delta_s = {}_i\delta$ (3a,b)

◆The hysteretic damper's installation stories：

・Characteristic value ${}_i\alpha_N$, Pseudo-brace stiffness ${}_iK_{bs} = {}_i\alpha_N\, {}_iK_{dR}$ (4)

・Specifications ${}_iK_{d1s} = ({}_i\alpha_N)^2 {}_iK_{d1}$, ${}_iK_{d2s} = ({}_i\alpha_N)^2 {}_iK_{d2}$, ${}_iF_{dys} = {}_i\alpha_N\, {}_iF_{dy}$ (5a,b,c)

Where ${}_iF_{dy}$ is yield shear force of hysteretic damper.

・Correspondence ${}_iF_{ds} = {}_i\alpha_N\, {}_iF_d$, ${}_i\delta_{ds} = {}_i\delta_d / {}_i\alpha_N$ (6a,b)

◆The viscous damper's installation stories：

・Characteristic value ${}_i\alpha_N$, Pseudo-brace stiffness ${}_iK_{bs} = {}_i\alpha_N\, {}_iK_{dR}$ (7)

・Specifications ${}_iC_{ds} = ({}_i\alpha_N)^2 {}_iC_d$, ${}_iK_{ds} = ({}_i\alpha_N)^2 {}_iK_d$ (8a,b)

・Correspondence ${}_iF_{ds} = {}_i\alpha_N\, {}_iF_d$, ${}_i\delta_{ds} = {}_i\delta_d / {}_i\alpha_{Ni}$ (9a,b)

α_N indicates the upper limit of the ratio of the horizontal component of the damper deformation to the story drift (hereinafter referred to as effective deformation ratio) [10], and K_{bs} of the simple model indicates the frame rigidity of the damper's installation position [11]. Fig. 3 shows the hysteresis curve of the pseudo-damper when a sinusoidal deformation is applied to an element in which a pseudo-brace and a pseudo-damper are connected in series. In Fig. 3(a), as the α_N decreases, the load loss of the VD decreases, and the height of the hysteresis curve decreases. In addition, as the pseudo-brace stiffness increases, the deformation loss of the VD decreases and the width of the hysteresis curve increases. In Fig. 3(b), the HD shows a similar trend.

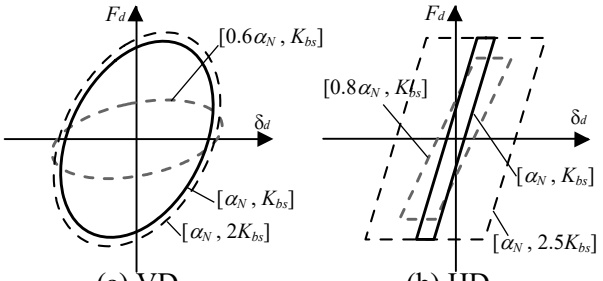

(a) VD (b) HD

Fig.3 Hysteresis curve of damper

2.2 Outline of the building for examination, outline of input ground motion, and response analysis results

A 30-story high-rise building (Fig. 4) was used to verify the proposed model [3]. Analysis was performed only in the X-direction. The natural period T_{f1} of the frame was 4.46 s. The frame remained elastic. The structural damping is a stiffness proportional type with 2% of T_{f1} of the frame.

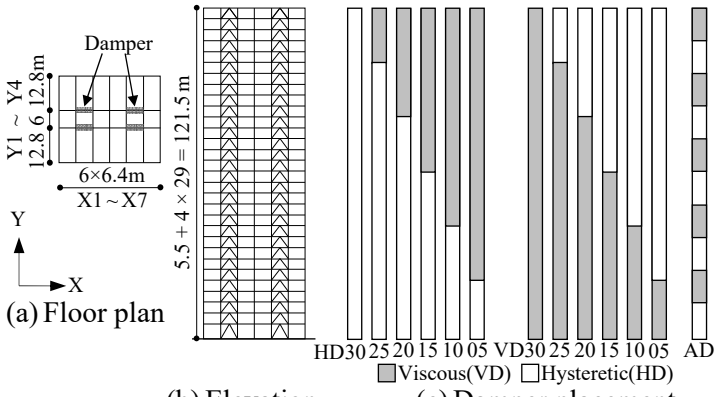

(a) Floor plan (b) Elevation (c) Damper placement

Fig.4 Outline of the 30th floor building models

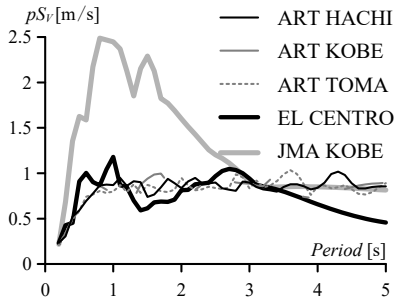

Fig.5 Pseudo-velocity response spectra of earthquake (h=5%)

The dampers were arranged continuously at Y2 and Y3. Recently, various damper arrangements have been proposed to increase damper efficiency. Therefore, we will consider many cases. The model with HDs on all floors is HD30. The model with VDs on all floors is VD30. Five models with HDs in the lower and VDs in the upper were used. Models with 25, 20, 15, 10, and 5 boundary stories were named HD25, HD20, HD15, HD10, and HD05, respectively. Five models with VDs in the lower and HDs in the upper were used. The models with 25, 20, 15, 10, and 5 boundary stories were named VD25, VD20, VD15, VD10, and VD05, respectively. A model in which HDs and VDs were arranged alternately every three stories was named AD. The amount of dumping for each model is shown in [3].

The input earthquake motions for the study comprised five waves, three simulated seismic waves with a velocity response spectrum of 0.8 m/s (h = 5%), and two observed waves normalized to a maximum velocity of 0.5 m/s. The phase characteristics of the simulated-seismic-waves were HACHINOHE 1968 EW

(ART HACHI), JMA KOBE 1995 NS (ART KOBE), and TOMAKOMAI 2003 NS (ART TOMA). The observed waves were EL CENTRO 1940 NS (EL CENTRO) and JMA KOBE 1995 NS (JMA KOBE). Fig. 5 shows the pseudo-velocity response spectrum ${}_pS_V$ ($h = 5\%$).

Fig. 6 shows the maximum story drift angle (${}_iR$) by HD15 ART HACHI, the maximum shear force (${}_iQ$), and the energy absorption by the damper (${}_iw_d$). Focusing on the maximum story drift angle and the maximum shear force, the previous model almost reproduced the member model, and the energy absorption by the damper of the previous model did not reproduce the response of member model in the boundary story. Only the response results of the ART HACHI of HD15 are presented in the following owing to space limitations.

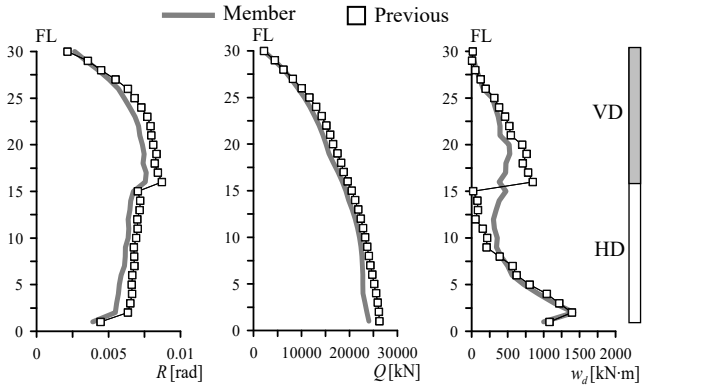

(a) Story drift angle (b) Story shear (c) Energy absorption by damper

Fig.6 Comparison of response (HD15, ART HACHI)

2.3 Cause analysis of the problem

In this section, the problems shown in the previous section are analyzed using damper history curves. Fig. 7 shows the hysteresis curves of the dampers installed on the 16th and 15th stories of HD15, which indicate a large difference in energy absorption between the previous and member models. The time axis is the portion where the amount of energy absorbed per unit time is large.

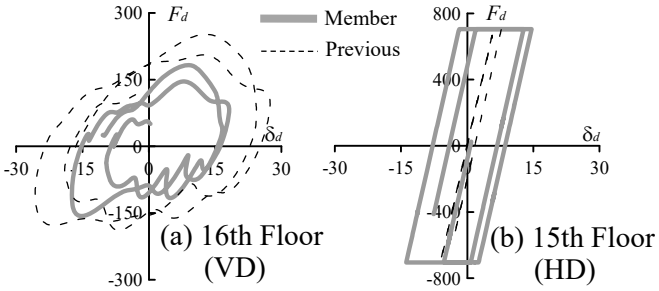

(a) 16th Floor (VD) (b) 15th Floor (HD)

Fig.7 Hysteresis curve of damper (HD15, ART HACHI)

First, the 16th story with VDs are shown below (Fig.7 (a)). Focusing on the maximum damper load, the previous model could not reproduce the member model. This was because α_N was overestimated, as shown in Section 2.2. Regarding the maximum damper deformation, the previous model could not reproduce the member model, and K_{bs} was underestimated. From Eq. (7), K_{bs} ($=\alpha_N K_{dR}$) decreases as α_N decreases, and α_N is assumed as not properly evaluated.

Next, the15th story with HDs are shown (Fig. 7 (b)). Focusing on the maximum damper load, the previous model could reproduce the member model. This was regarded as an appropriate evaluation of α_N. Meanwhile, focusing on the maximum damper deformation, the previous model could not reproduce the

member model because the previous model exhibited a large deformation loss. This was because K_{bs} was underestimated, as shown in Section 2.2.

The α_N of stories with VDs that was not evaluated appropriately is shown below. As described above, because α_N is the upper limit of the effective deformation ratio, we confirmed whether the upper limit of the effective deformation ratio of the stories with VDs matches α_N. Fig. 8 shows the distribution of the effective deformation ratio α_e of HD15 with only HDs partially arranged. Additionally, Fig. 8 shows the apparent effective deformation ratio of the frame. The apparent damper deformation of the nondamper stories was calculated using the damper deformation of the elastic spring with the stiffness set to zero. From Fig. 8, it can be confirmed that the effective deformation ratio of the nondamper stories (16–30th story) in the model with partially arranged HDs is smaller than that of the frame. Therefore, it is necessary to improve the α_N of the VD installation stories of the combination system.

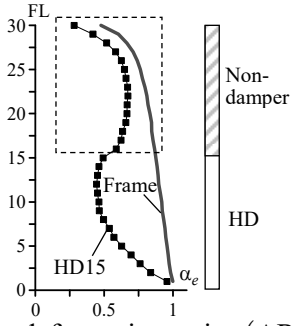

Fig.8 Effective deformation ratio（ART HACHI）

Next, the K_{bs} of stories with HDs is shown. As described above, K_{bs} is the frame rigidity of the part where the damper is installed; therefore, the properties of bending deformation of the frame are shown below. Fig. 9 shows the time history of the story drift ${}_i\delta$, damper deformation ${}_i\delta_d$, bending deformation ${}_i\delta_m$ (=${}_i\delta$-${}_i\delta_d$), and damper load ${}_iF_d$ of HD30 and HD15. Representatively, the 15th story with HDs and 16th story with VDs are shown. ${}_i\delta$, ${}_i\delta_d$, and ${}_i\delta_m$ are normalized by the maximum story drift ${}_i\delta$ (max) of each story, and ${}_iF_d$ is normalized by the maximum value ${}_iF_d$ (max).

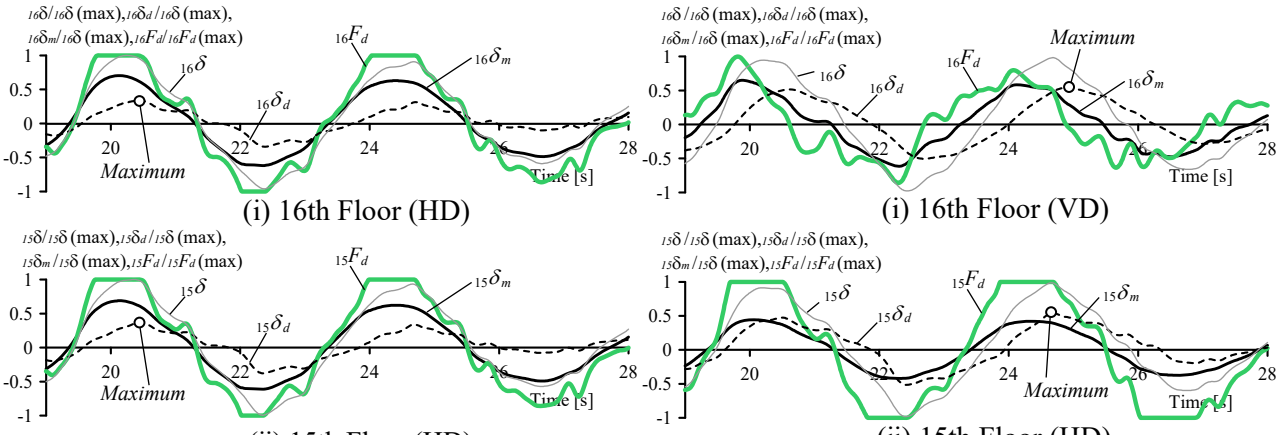

(i) 16th Floor (HD) (i) 16th Floor (VD)

(ii) 15th Floor (HD) (ii) 15th Floor (HD)

(a) HD30 (b) HD15

Fig.9 Time history (HD15, ART HACHI)

As shown in Fig. 9 (a), in the HD30 with HDs installed in all stories, the damper load of the 15th and 16th stories is maximized when the damper deformation is maximum. Furthermore, the bending deformation is almost in phase with the damper load. As the frame is deformed, the damper bears the shear force, and the reaction force induces the axial force of the column. Moreover, the ratio of the total bending deformation to the story drift increases [12]. Focusing on HD15 shown in Fig.9 (b), the HD load is the maximum when the

damper deformation is the maximum. However, for the case where the VD is dependent on velocity, the damper load is almost zero when the damper deformation is the maximum. Furthermore, the HD15 bending deformation of the 15th story is almost in phase with that of HD30, but the bending deformation amplitude of HD15 is smaller than that of HD30. This can be confirmed from the distribution of the ration of the maximum bending deformation to the maximum story drift (bending deformation ratio), shown in Fig.10. The phase of HD and VD loads are different, and the bending deformation ratio of the 10–15th story of HD15 is smaller than that of HD30. Therefore, it is necessary to improve the K_{bs} of the HD installation location of the combination system.

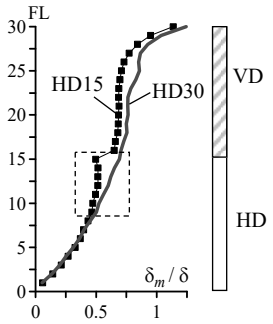

Fig.10 Bending deformation ratio（ART HACHI）

3. Proposal of improvement method for problem

To create a simple model that can be used for the combination system, this paper proposes a method for correcting the parameters obtained from state *N* and *R* analyses. This method is illusrated in Fig. 2. In addition to the existing methods of state *N* (Fig. 2 (b)) and state *R* analyses (Fig. 2 (c)), a static analysis of two cases shown in Figs. 2 (d) and 2 (e) (State *pN* and *pR* analysis, respectively) was additionally conducted, characteristic values were calculated, and the existing characteristic values were corrected using these characteristic values. An outline of states *pN* and *pR* is as follows.

First, to improve "problem ①" (When the HD is partially arranged in the height direction, the effective deformation ratio of the nondamper stories is reduced compared with the frame), the ${}_i\alpha_N$ of the VD's installation stories was corrected using the characteristic values obtained from state *pN*. State *pN* (Fig.2 (d), partial no-damper) is a model in which in which elastic springs are placed only in the HD's installation stories. The characteristic value ${}_i\alpha_{pN}$ of the i-story VD installation was calculated using Eq. (10). The stiffness of the elastic spring is the initial stiffness of the HD. The load in the static analysis is based on the Ai distribution.

$$ {}_i\alpha_{pN}(K_d) = {}_i\delta_{dpN} / {}_i\delta_{pN} \tag{10} $$

where the lower right subscripts *pN* indicate the calculated values of states *pN*; (K_d) indicates that the value varies depending on the initial stiffness K_d of the HD; ${}_i\alpha_{pN}$ depends on the amount of HD and the number of damper installation stories (shown in section 4.1)

Next, to improve "the problem ②" (Because the phase of HD and VD loads are different, the frame rigidity of the HDs in the combination system increases compared with the model with HDs on all stories); the ${}_iK_{dR}$ of the HD's installation position was corrected using the characteristic values obtained from state *pR*. State *pR* (Fig. 2 (d), partially rigid damper) is a model in which an elastic spring with extremely high rigidity is placed only on the HD's installation position. The frame rigidity ${}_iK_{dpR}$ of the HD's installation position was calculated by Eq. (11). The load in the static analysis is based on the Ai distribution.

$$ {}_iK_{dpR} = {}_iF_{dpR} / {}_i\delta_{pR} \tag{11} $$

where the lower right subscripts *pR* indicate the calculated values of states *pR*; ${}_iK_{dpR}$ does not depend on the amount of damper but on the number of VD stories.

Fig. 11 shows the procedure for the conversion from a member model to an equivalent shear spring model. The parameters were calculated by conducting a static analysis of the building frame in four states (states *N*, *R*, *pN*, and *pR*), and each specification was set as follows using the characteristic values.

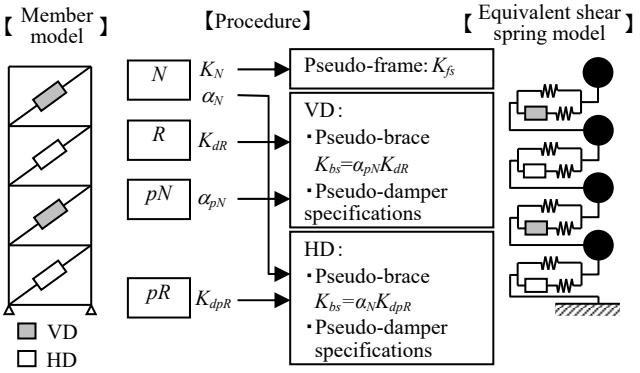

Fig.11 Procedure for the conversion from member model to equivalent shear spring model

◆Frame：

・Pseudo-frame rigidity ${}_iK_{fs} = {}_iK_N$ (12)

・Correspondence ${}_iF_s = {}_iF$, ${}_i\delta_s = {}_i\delta$ (13a,b)

◆The hysteretic damper's installation stories：

・Characteristic value ${}_i\alpha_N$, Pseudo-frame rigidity ${}_iK_{bs} = {}_i\alpha_N\,{}_iK_{dpR}$ (14)

・Specifications ${}_iK_{d1s} = ({}_i\alpha_N)^2{}_iK_{d1}$, ${}_iK_{d2s} = ({}_i\alpha_N)^2{}_iK_{d2}$, ${}_iF_{dys} = {}_i\alpha_N\,{}_iF_{dy}$ (15a,b,c)

・Correspondence ${}_iF_{ds} = {}_i\alpha_N\,{}_iF_d$, ${}_i\delta_{ds} = {}_i\delta_d / {}_i\alpha_N$ (16a,b)

◆The viscous damper's installation stories：

・Characteristic value ${}_i\alpha_{pN}$, Pseudo-frame rigidity ${}_iK_{bs} = {}_i\alpha_{pN}\,{}_iK_{dR}$ (17)

・Specifications ${}_iC_{ds} = ({}_i\alpha_{pN})^2{}_iC_d$, ${}_iK_{ds} = ({}_i\alpha_{pN})^2{}_iK_d$ (18a,b)

・Correspondence ${}_iF_{ds} = {}_i\alpha_{pN}\,{}_iF_d$, ${}_i\delta_{ds} = {}_i\delta_d / {}_i\alpha_{pNi}$ (19a,b)

4. Application of the proposed method and verification of accuracy

4.1 Properties of ${}_i\alpha_{pN}$ and ${}_iK_{bs}$

Fig. 12 shows the distributions of ${}_i\alpha_{pN}$ and ${}_iK_{bs}$ for 13 models with different damper arrangements. ${}_iK_{bs}$ was normalized by ${}_iK_{fs}$. An elastic spring corresponding to the initial stiffness of ${}_1\alpha_{dy} = 0.025$ was used in the calculation of ${}_i\alpha_{pN}$. Because the ${}_i\alpha_{pN}$ of the HD's installation stories is not corrected, it indicates ${}_i\alpha_N$ From Fig. 12 (a), it can be confirmed that the ${}_i\alpha_{pN}$ of the VD's installation stories in the combination system shows a smaller value than that of HD30. That is, it can be confirmed that state *pN* can reduce the upper limit of the effective deformation ratio of the VD's installation stories. Moreover, it can be confirmed that the ${}_i\alpha_{pN}$ of the VD's installation stories of the combination system decreases, as the number of HD's installation stories increases. Furthermore, it has been confirmed that ${}_i\alpha_{pN}$ decreases with the amount of HD.

From Fig. 12 (b), it can be confirmed that the iKbs of the HD's installation stories of the combination system increases compared with that of HD30. In particular, iKbs protrudes in the boundary stories. State pR can increase the frame rigidity of HD's installation position.

4.2 Accuracy verification by time history analysis

This section shows the verification results of whether the proposed model can reproduce the results of time-history analysis of the member models. Figs. 13 and 14 show the maximum story drift angle ($_iR$) and energy absorption by the damper ($_iw_d$) on each story in the ART HACHI wave. The responses of states *N*, *R*, *pN*, and *pR* are shown as well. Focusing on the maximum story drift angle, no significant difference is observed between the proposed and previous models in all 13 types. Focusing on the energy absorption by the damper, the previous model cannot reproduce the member model near the boundary layer in all 13 types. Meanwhile, the energy absorption by damper ($_iw_d$) of the proposed model accurately reproduces the member model. Furthermore, as shown by the hysteresis curve in Fig. 15, it can be confirmed that the proposed model is more reproducible than the previous model.

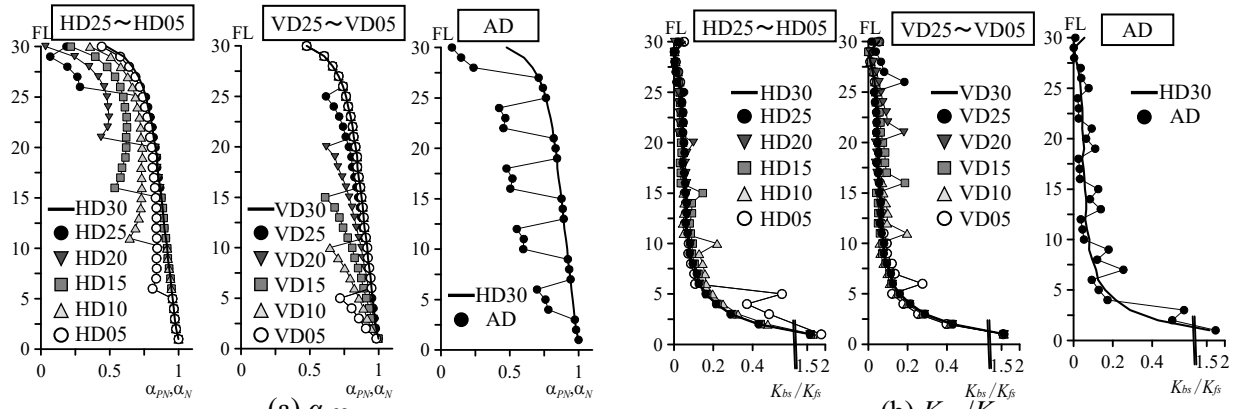

(a) α_{pN} (b) K_{bs}/K_{fs}

Fig.12 Comparison of distribution of α_{pN} and K_{bs}

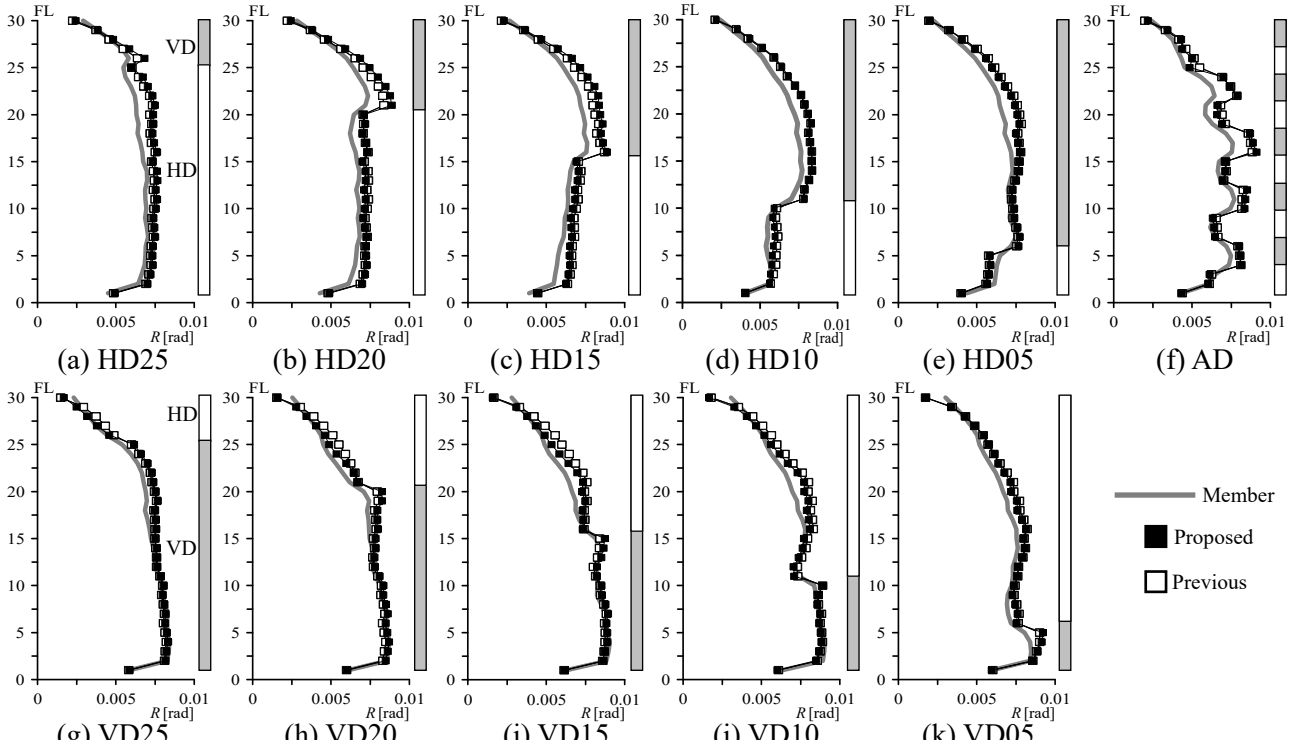

(a) HD25 (b) HD20 (c) HD15 (d) HD10 (e) HD05 (f) AD

(g) VD25 (h) VD20 (i) VD15 (j) VD10 (k) VD05

Fig.13 Comparison of story drift angle (ART HACHI)

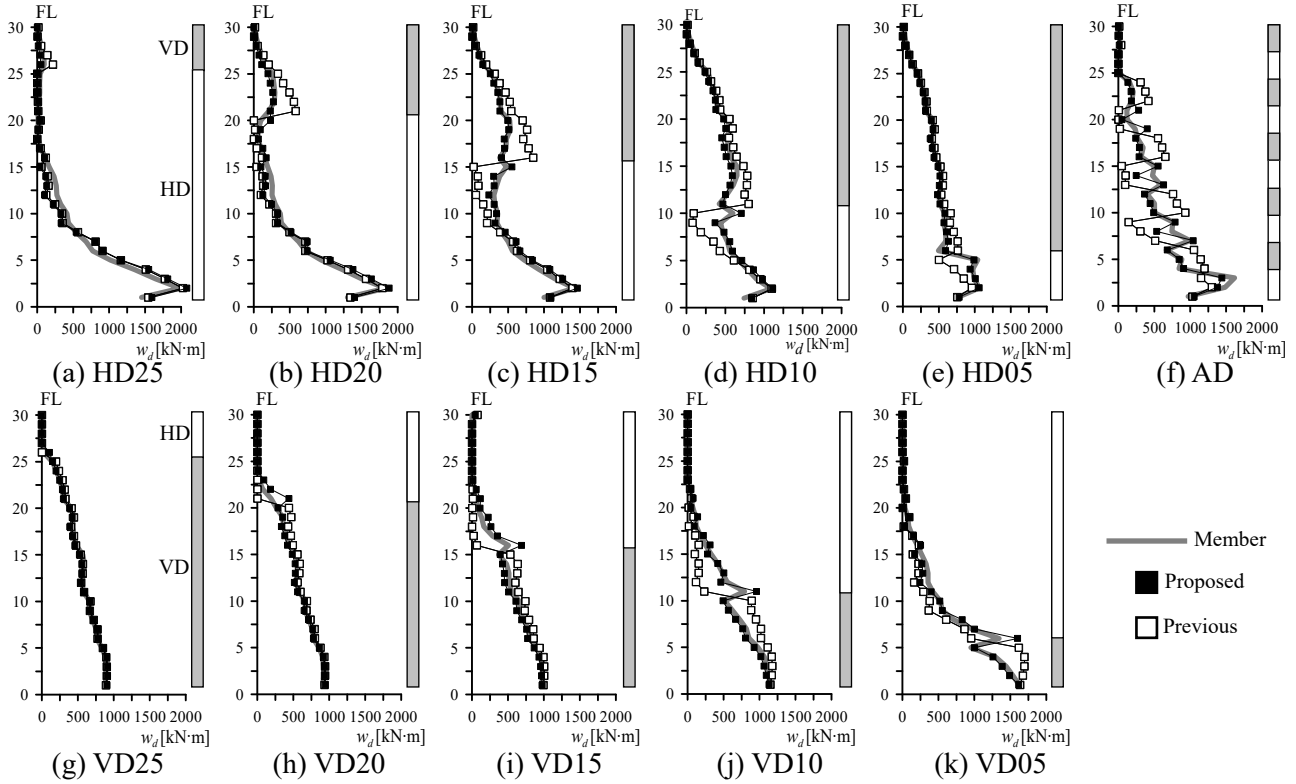

Fig.14 Comparison of energy absorption by damper (ART HACHI)

Next, Figs. 16 and 17 show the comparison of the responses of the member and simple models in the case of the JMA KOBE wave. HD15, VD15, and AD are shown as representative responses. Focusing on the story drift angle (*iR*), both models are affected by higher modes; therefore, the simple model is larger than the member model in the upper layer, and the proposed and previous models cannot reproduce the member model. Focusing on the energy absorption by the damper ($_i w_d$), the proposed model roughly reproduces the distribution shape of the member model, but the accuracy is inferior compared to that of the ART HACHI wave.

Furthermore, it has been confirmed that the proposed model is highly useful for the yield shear coefficient $_1\alpha_{dy}$ = 0.005, 0.015, and 0.035 of the HD.

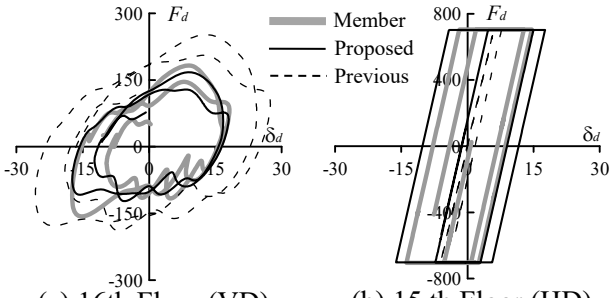

Fig.15 Hysteresis curve of damper (HD15, ART HACHI)

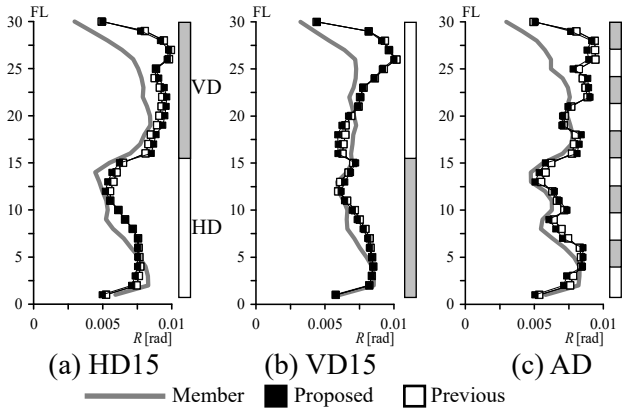

Fig.16 Comparison of story drift angle (JMA KOBE)

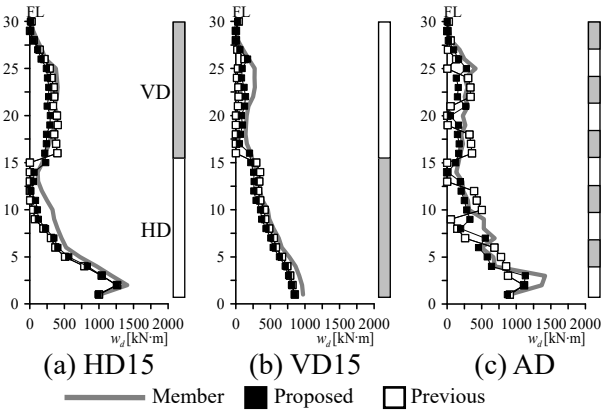

Fig.17 Comparison of energy absorption by damper (JMA KOBE)

5. Conclusion

This paper presents a simple modelling method of the continuous arrangement of HDs and VDs in buildings. Accuracy was verified based on a 30-story super-high-rise steel structure building with HDs and VDs installed in a brace shape. The findings obtained are shown below.

1) Previous methods did not consider two problems. “Problem ①”: The upper limit of the effective deformation ratio (maximum value of damper deformation/maximum value of story drift) of the VD’s installation stories decreased. “Problem ②”: Because a phase difference occurred between the HD and VD loads, the bending deformation of the combination system was relaxed.

2) To improve the problems shown in 1), we proposed adding state *pN* and *pR* analyses to the previous method. State *pN* improved “problem ①,” whereas state *pR* improved “problem ②.”

3) The proposed model reproduced the results of time-history analysis of member models accurately for various damper arrangements, damper amounts, and seismic waves.

The proposed model was applied to the case where the VD load was small when the damper deformation was the maximum. Therefore, in future studies, verification must be performed for the case where the VD load is large when the damper deformation is the maximum.

Acknowledgements

The authors are grateful to Keisuke Yoshie (Nikken Sekkei Ltd.), Mitsuru Miyazaki (Oiles Corporation), Kazuhiko Sasaki (Oiles Corporation), and Yuichi Iwasaki (Oiles Corporation) for their invaluable advice and cooperation in this research.

References

[1] Atsumi T., Kitamura H., Ishii M. and Uramoto H.: Vertical Distribution of Hysteretic and Velocity-Dependent Dampers for High-Rise Steel Structure (Part 1, 2), Summaries of Technical Papers of Annual Meeting, Architectural Institute of Japan, B-2, pp. 763-766, 2006. 7 (in Japanese)

[2] Ishida T., Sato D., Kitamura H., Sasaki K., Miyazaki M., Yoshie K., Ishii M. and Fujita T.: Shaking Table Tests of 10th Story Steel Model Using Combinations of Hysteretic and Viscous Dampers, Journal of Structural Engineering, Vol. 55B, pp. 507-515, 2009. 3 (in Japanese)

[3] Soeta K., Sato D., Kitamura H., Ishii M., Yoshie K., Miyazaki M., Sasaki K. and Iwasaki Y.: Influence of the Continuous Arrangement of Hysteretic Damper and Viscous Damper on Vibration Control Effect of High-rise Building, AIJ Journal of Technology and Design, No. 39, pp. 477-482, 2012. 6 (in Japanese)

[4] Kitamura H.: Seismic Response Analysis Methods for Performance Based Design (Second edition), SHOKOKUSYA Publishing Co., Ltd., 2009. 4 (in Japanese)

[5] Kasai K. and Iwasaki K.: Reduced Expression for Various Passive Control Systems and Conversion to Shear Spring Model, Journal of Structural and Construction Engineering (Transactions of AIJ), No. 605, pp. 37-46, 2006. 7 (in Japanese)

[6] Ishii M. and Kasai K.: Shear Spring Model for Time History Analysis of Multi-story Passive Controlled Buildings, Journal of Structural and Construction Engineering (Transactions of AIJ), No. 647, pp. 103-112, 2010. 1 (in Japanese)

[7] Ishii M., Kitamura H., Wada A., and Kasai K.: A Study on Analytical Model for Frames Using Viscoelastic Dampers, Journal of Structural and Construction Engineering (Transactions of AIJ), No. 531, pp. 55-62, 2000. 5 (in Japanese)

